A Wearable Vital Signs Monitor at the Ear for Continuous Heart Rate and Pulse Transit Time Measurements

Eric S. Winokur [Student Member, IEEE], **David Da He [Student Member, IEEE]**, and **Charles G. Sodini [Fellow, IEEE]**

Massachusetts Institute of Technology, Cambridge, MA 02139 USA.

Abstract

A continuous, wearable and wireless vital signs monitor at the ear is demonstrated. The device has the form factor of a hearing aid and is wirelessly connected to a PC for data recording and analysis. The device monitors the electrocardiogram (ECG) in a single lead configuration, the ballistocardiogram (BCG) with a MEMS triaxial accelerometer, and the photoplethysmograms (PPG) with 660nm and 940nm LED sources and a static photocurrent subtraction analog front end.

Clinical tests are conducted, including Valsalva and head-up tilt maneuvers. Peak timing intervals between the ECG, BCG and PPG are extracted and are shown to relate to pre-ejection period and mean arterial blood pressure (MAP). Pulse Transit Time (PTT) extracted from cross-correlation between the PPG and BCG shows improved results compared to the pulse arrival time (PAT) method for tracking changes in MAP.

I. Introduction

Cardiovascular disease (CVD) affects more than 80 million people as of 2008 and is the leading cause of death in the U.S. [1]. In 2008, costs associated with CVD were $297.7 billion, and by 2030, costs are expected to reach $1.117 trillion per year for CVD in the U.S. alone [1]. To help reduce these costs, there is a push to change the current hospital-centric, reactive healthcare delivery system to one that focuses on early detection and diagnosis through extended, personalized monitoring [2] [3].

Continuously monitoring vital signs such as heart rate (HR) and heart intervals can provide the data necessary for early diagnosis of CVD [4]. Several groups have designed measurement systems to monitor many of these vital signs for personalized health care. Guo *et al*. designed a wearable vital signs monitor with a chest belt for electrocardiography (ECG) and an ear-worn probe for photoplethysmography (PPG) [5]. They measured heart rate, peripheral oxygen saturation (SpO_2) and systolic blood pressure using the pulse-arrival time (PAT) method. Pinheiro *et al*. measured the PPG at the finger, the ECG at the chest and the ballistocardiogram (BCG) from a chair for heart rate variability (HRV), HR, PAT and SpO_2 measurements [6].

Here, we demonstrate a continuous, wearable and wireless vital-sign monitor worn at the ear in the form factor of a hearing aid. The ear location is chosen because it is a natural anchoring point, and it is discreet since the device can be partially hidden by hair and the ear [7]. It is also chosen so that all physiological signals can be acquired from one location for improved patient compliance. The monitor measures single lead ECG, BCG, and PPG. These physiological signals allow the monitor to measure heart rate from three independent sources, and blood oxygenation. Additionally, information embedded in the peak timings between the signals has been shown to correlate to the preejection period (PEP), heart contractility, stroke volume, cardiac output and mean arterial blood pressure, the last of which will be discussed in this paper [8 – 11].

II. Measuring Physiological Signals at the Head

A. Head Ballistocardiogram (BCG)

The BCG is a measure of the body's mechanical reaction to the blood ejected during systole and is traditionally measured by having a subject lie on a low-friction bed [8]. As noted in [9], the head BCG recoil is in the head-to-foot axis, which is consistent with the principal blood-volume shift during cardiac ejection. These movements are typically 10 mG_{p-p}. To measure the BCG, we employ a Bosch BMA180 MEMS triaxial accelerometer with a 9 Hz bandwidth, 14 bit resolution, and ± 2G range [9]. The low SNR of the BCG signal requires this measurement to be taken at rest.

B. Head Electrocardiogram (ECG)

Due to the conductive nature of the body, the ECG can be measured in an attenuated form at different locations away from the heart. A single-lead ECG is used, with one electrode placed on the mastoid bone, and the other on the neck. The ECG front-end circuit is shown in Fig. 1 [9]. The instrumentation amplifier (IA) has an adjustable gain to amplify QRS complexes on the order of 30 – 40μV_{p-p}. The low SNR of the ECG signal requires this measurement to be taken at rest.

C. Head Photoplethysmogram (PPG)

The head PPG is taken in reflectance mode, with light reflecting off the mastoid bone to photodiodes in the same plane as the LED light sources. The PPG has a small pulsatile component, usually between 0.25 – 1% of a large static component [12]. This large static current presents many challenges for low-voltage, single-supply systems. Typically, reducing the LED drive current can maintain the output of the transimpedance amplifier (TIA) within the supply rails, at the expense of lower signal-to-noise ratio (SNR). Alternatively, reducing the transimpedance of the feedback element will achieve the same result.

Wong *et al*. developed a static photocurrent subtraction circuit by using an error amplifier in feedback with the transimpedance amplifier to drive a current source into the cathode of the photo-diodes [13]. However, the frequency response of the TIA changes due to the amount of static photocurrent subtracted, and can reduce the bandwidth to unacceptably low levels.

Tavakoli utilized a log-amp in the front end to increase dynamic range, requiring a full signal path for each PPG wavelength [12].

To address these concerns, a new photoreceptor circuit has been designed, in which the photodiodes are forward biased (Fig. 2). A digital-to-analog converter (DAC) is used to generate a reference voltage V_{ref} at the positive terminal of the TIA. The amount of static photocurrent subtracted from the PPG is determined by the diode equation:

$$I_F = I_s \left(e^{\frac{V_D}{V_T}} - 1 \right) \quad (1)$$

where I_F is the forward diode current, I_s is the reverse bias saturation current, V_D is the voltage across the diode and V_T is the thermal voltage kT/q. Due to the virtual ground of the TIA op-amp, V_{ref} is equal to V_D and therefore sets the forward biased diode current. The photocurrent I_{ph}, which flows in the reverse direction of I_F, is set through feedback from the microcontroller unit (MCU) to the LED driver, so that the remaining current I_{OA} is sufficiently small for the opamp to supply. According to Kirchoff's Current Law (KCL), the current into a node, must equal the current out:

$$I_{OA} = I_F - I_{ph} \quad (2)$$

$$\frac{-V_{ref}}{R_F} \leq I_{OA} \leq \frac{V_{DD}}{R_F} \quad (3)$$

The exponential nature of (1) allows the total amount of subtracted photocurrent to be large as given by (2), with the current steps being defined by the resolution of the DAC. A 16-bit R-2R ladder DAC (Analog Devices AD5541A) has sufficient resolution for this application and was used in this implementation.

Feedback from the MCU (Texas Instruments MSP430) is used to control the LED drive currents and DAC voltage. If the LED drive current becomes too large, the MCU can lower V_{ref} to reduce power consumption of the system. Fig. 3 shows the ECG, BCG and PPG (red light only) signals simultaneously measured at the head. LED optical output power during these experiments was limited to between 0.027 and 0.068 lumens.

III. System Description

The system consists of the BCG accelerometer, the ECG front end, the PPG front end, a power management circuit, a microcontroller, a wireless transmitter and receiver, the PC software and the mechanical housing.

The BCG, ECG and PPG components have been described in Section II. Power is supplied by a 3V lithium coin cell battery (Panasonic CR2032) and the rest of the power management circuitry is described in [9].

The MCU shuttles the continuous real time BCG, ECG and PPG data to the 2.4 GHz low-power wireless transmitter (Texas Instruments CC2500). The raw data is displayed in MATLAB in real time for visual feedback during testing.

The mechanical housing of the device is modified from a hearing aid housing, which consists of a plastic shell that is attached to an ear-bud. The custom designed Rigid – FLEX PCB is 0.5 mm thick and contains a 5.08cm flexible connector for the PPG subsystem to fold over and interface with the mastoid bone. The PPG sensor has 660nm and 940nm LED sources surrounded by 4 photodiodes (Advanced Photonix PD-C160SM). Fig 4 shows the entire prototype system anchored to the ear.

IV. Determining Heart Intervals Using Simultaneous ECG, BCG, and PPG

Several heart intervals can be determined via the three physiological signals measured with the vital signs monitor; Pre-ejection period (PEP), defined as the electro-mechanical delay between the onset of ECG's Q wave and the time when the aortic valve opens [11]; pulse arrival time (PAT), defined as the time between the Q wave and the arrival of the pulse wave to a location on the body [11]; pulse transit time (PTT), defined as the time it takes for a pulse wave to travel from one location to another location in the vasculature [11].

A. ECG & BCG: PEP

The vital-signs monitor in practice estimates the PEP as the delay between the R wave of the ECG, and the principal wave of the BCG (the J wave). This measurement includes the PEP, as well as a small portion of PTT, as the J wave motion is due to the blood pulse moving around the aortic arch and down the descending aorta [9]. The PEP contains information related to the contractility of the heart, stroke volume, cardiac output, and autonomic responses [10].

B. ECG & PPG: PAT

PAT is measured in practice as the delay between the R wave of the ECG and diastole of the PPG [14]. PAT includes both PEP and PTT intervals. Information from the PAT has been used to estimate cuff-less mean arterial blood pressure (MAP). However many inaccuracies may arise due to the changes in PEP, which are not necessarily correlated with MAP [14]. This will be discussed further in Section V.

C. PAT – PEP = PTT

When subtracting PEP from PAT, the remaining signal is purely PTT. MAP has been empirically related to PTT via a negative logarithmic relationship through a long tube pulse wave velocity model [15] [16]:

$$MAP = A - B \times ln\left(PTT\right) + P_{hydro} \quad (4)$$

In Eq. (4), *A* is a constant dependent on the elastic properties of the vasculature and the distance the pulse wave has traveled. *B* is also a constant dependent on elastic properties of the vasculature and *Phydro* is the hydrostatic pressure due to gravity [15][16]. *Phydro* becomes zero when the subject is supine. Compared to measuring PTT from a finger PPG,

calibration for the vital signs monitor should be greatly reduced since the head is almost always upright or level compared to the heart [5]. The ability to subtract PEP accurately from this equation removes one of the large error sources associated with transit-derived ABP [11] [14].

V. Measured Changes in Heart Intervals due to Hemodynamic Maneuvers

Fig. 5 shows continuous blood pressure from a Finapres monitor, as well as -ln(PTT), R-J interval and -ln(PAT) derived from signals measured simultaneously from the vital signs monitor. All signals were manually annotated to ensure accuracy.

During the intervention, the subject was at rest for 50s, and then performed a Valsalva for approximately the next 20s, and finally was at rest again for the next 50s. The change in ABP observed during the Valsalva maneuver corresponds to the changes noted in [17]. A qualitative correlation between Finapres MAP and -ln(PTT)) is discernible, whereas no such qualitative correlation is seen between MAP and -ln(PAT). The lack of qualitative correlation from -ln(PAT) is due to the change in PEP during the maneuver, moving in the opposite direction as PTT. As the maneuver begins, PEP is shown to lengthen, whereas after a brief lengthening of PTT, the autonomic response causes vasoconstriction, thus reducing the PTT interval.

Fig. 6 compares transit derived MAP and Finapres MAP. Solving for *A* and *B* in (4) yields 44 and 0.05 respectively. The mean error is -0.07 mmHg with a standard deviation of 3.64 mmHg.

Fig. 7 shows simultaneously measured PTT, PAT and R-J intervals during a head-down tilt maneuver (from 75° head-up tilt to supine). The PTT is measured by cross-correlating and averaging the filtered BCG and derivative PPG; the PAT is measured by cross-correlating and averaging the filtered ECG and the derivative PPG; the R-J interval is measured by cross-correlating and averaging the filtered ECG and BCG waveforms [9]. During the first portion of the measurement, the subject is tilted at 75°. After three minutes, the subject is lowered to supine for another three minutes. The decrease in R-J interval is caused by the influx of venous return as the body goes to the supine position [10] [18]. The increase in -ln(PTT) and -ln(PAT) is due to the increase in circulatory blood as venous pooling is no longer occurring, and qualitatively correlates to expected changes in blood pressure [19] [20]. Here, -ln(PAT) correlates to the expected change in blood pressure because the PEP and PTT intervals are both changing in the same direction (decreasing).

VI. Conclusions and Future Work

A wearable and wireless vital-signs monitor at the ear has been demonstrated. The portable device measures the ECG, BCG and PPG, all from a single area behind the ear. R-J interval and –ln(PTT) have been shown to correlate to preejection period and arterial blood pressure, respectively.

Future work to improve the power consumption and accuracy of the measurements will occur by changing the radio to BlueTooth Low Energy, designing custom integrated circuits for the ECG and PPG front ends, and improving the mechanical design of the device.

Acknowledgment

References

1. Veronique RL, et al. Heart Disease and Stroke Statistics - 2012 Update: A Report from the American Heart Association. Circulation. Dec.2011

2. Troster G. The Agenda of Wearable Healthcare. IMIA Yearbook of Med. Info. 2005: Ubiquitous Health Care Systems. 2004:125–138.

3. Teng X-F, T Zhang Y- Poon CCY, Bonato P. Wearable Medical Systems for p-Health. IEEE Reviews in Biomedical Engineering. 1:62–74, 2008. [PubMed: 22274900]

4. Lymberis A. Smart Wearable Systems for Personalised Health Management: Current and Future Challenges. IEEE EMBC. :3716–3719, 2003.

5. Guo DG, Tay FEH, Xu L, Nyan MN, Chong FW, Yap KL, Xu B. A Long-term Wearable Vital Signs Monitoring System using BSN. 11th EUROMICRO Conference on Digital System Design Architectures, Methods and Tools. Sep 3-5.2008 :825–830.

6. Pinheiro E, Postolache O, Girao P. Pulse arrival time and ballistocardiogram application to blood pressure variability estimation. IEEE International Workshop on Medical Measurements and Applications. May 29-30.2009 :132–136.

7. He D, Winokur ES, Heldt T, Sodini CG. The Ear as a Location for Wearable Vital Signs Monitoring. IEEE EMBC. 2010:6389–6392.

8. Starr I, Rawson AJ, Schroeder HA, Joseph NR. Studies on the Estimation of Cardiac Output in Man, and of Abnormalities in Cardiac Function, from the Heart's Recoil and the Blood's Impacts; the Ballistocardiogram. The American Journal of Physiology. 1939; 127:1–28.

9. He D, Winokur ES, Sodini CG. A Continuous, Wearable, and Wireless Heart Monitor using Head Ballistocardiogram (BCG) and Head Electrocardiogram (ECG). IEEE EMBC. 2011:4739–4732.

10. Etemadi M, Inan OT, Wiard RM, Kovacs GTA, Giovangrandi L. Non-Invasive Assessment of Cardiac Contractility on a Weighing Scale. IEEE EMBC. :6773–6776, 2009.

11. Zhang G, Xu D, Olivier NB, Mukkamala R. Pulse arrival time is not an adequate surrogate for pulse transit time in terms of tracking diastolic pressure. IEEE EMBC. :6462–6464, 2011.

12. Tavakoli, MD. PhD Thesis. MIT; Cambridge, MA: 2006. An Analog VLSI Front End for Pulse Oximetry.

13. Wong AKY, P Pun K- Zhang Y-T, Leung KN. A Low-Power CMOS Front-End for Photoplethysmographic Signal Acquisition with Robust DC Photocurrent Rejection. IEEE Trans. On Biomed. Cir. And Sys. Dec; 2008 2(4):280–288.

14. Fung P, Dumont G, Ries C, Mott C, Ansermino M. Continuous Noninvasive Blood Pressure Measurement by Pulse Transit Time. IEEE EMBC. 2004:738–741.

15. Chen W, et al. Continuous Estimation of Systolic Blood Pressure Using the Pulse Arrival Time and Intermittent Calibration. IEEE Comput. Med. Biol. Eng. 2000; 38:569–574.

16. Shaltis P, Reisner A, Asada H. A Hydrostatic Pressure Approach to Cuffless Blood Pressure Monitoring. IEEE EMBC. 2004:2173–2176.

17. Heldt, T. Ph.D. dissertation. Harvard-MIT Division of Health Sciences and Technology; Cambridge, MA: 2004. Computational Models of Cardiovascular Response to Orthostatic Stress.

18. Stafford RW, Harris WS, Weissler AM. Left Ventricular Systolic Time Intervals as Indices of Postural Circulatory Stress in Man. Circulation. 1970; 41:485–492. [PubMed: 5415986]

19. Costanzo, LS. Physiology. 4th Edition. Elsevier; 2010.

20. Heldt T, Oefinger MB, Hoshiyama M, Mark RG. Circulatory Response to Passive and Active Changes in Posture. IEEE Computers in Cardiology. 2003; 30(263):263–266.
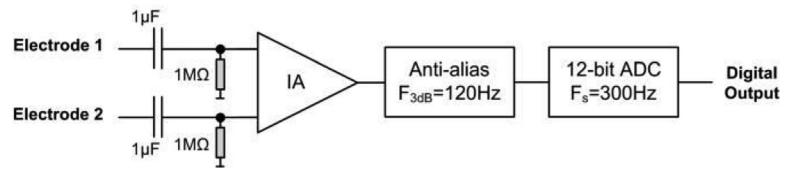
Fig. 1.
The head ECG front end circuit. IA: instrumentation amplifier; ADC: analog-to-digital converter.
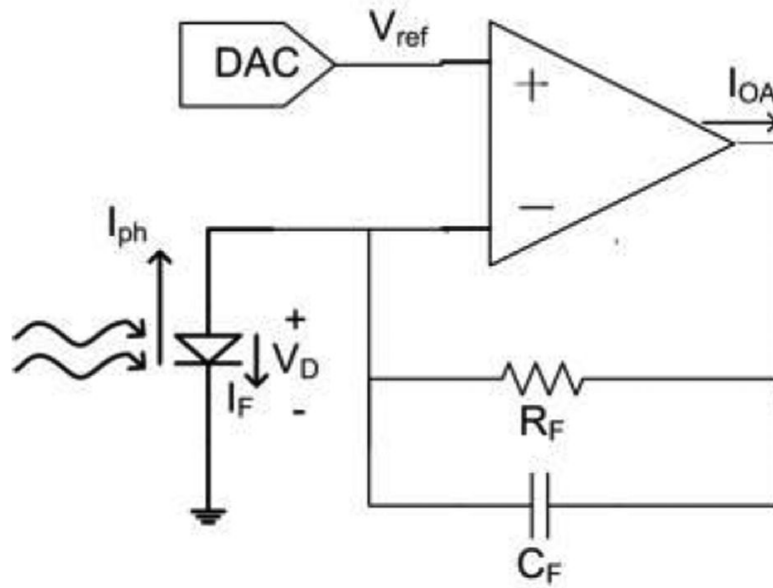
Fig. 2.
PPG front end with forward biased photo-diodes. The forward diode current I_F subtracts a static amount of photocurrent from I_{ph}, which increases the dynamic range of the front end.
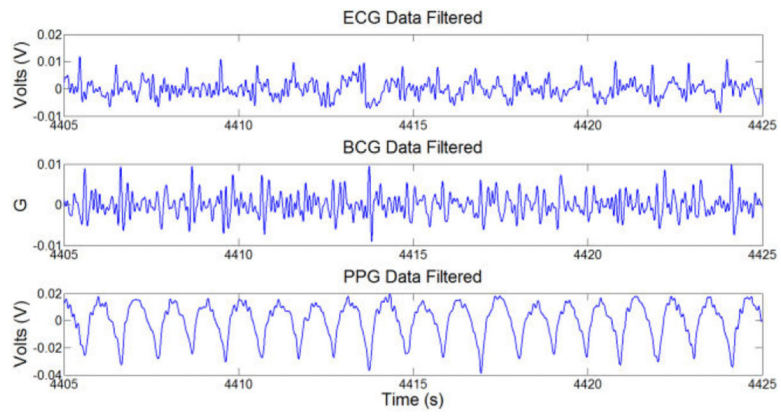
Fig. 3.
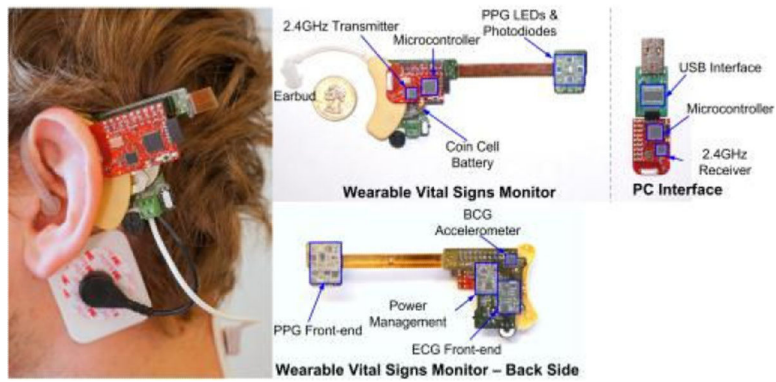ECG, BCG, and PPG data collected simultaneously at the head

Fig. 4.
Left: The wearable vital signs monitor worn at the ear. Center top: Front side of the monitor with MSP430, radio, battery and PPG sensor outlined. Center bottom: Back side of the monitor with PPG and ECG front ends, power management and accelerometer outlined. Right: The USB interface that allows the device to interface with MATLAB.
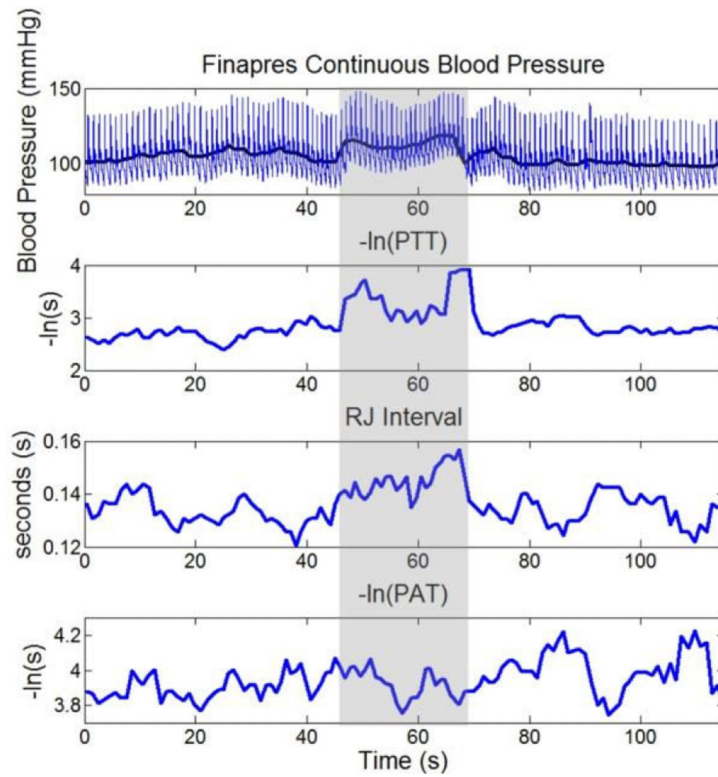
Fig. 5.
Top panel: Finapres continuous BP data before, during, and after a Valsalva maneuver. The bold line corresponds to MAP. 2nd panel: -ln(PTT), averaged over 5 beats showing qualitative correlation to MAP. 3rd panel: RJ Interval during the maneuver averaged over 5 beats. 4th panel: -ln(PAT), averaged over 5 beats not showing significant qualitative correlation to MAP due to the change in PEP moving in the opposite direction as PTT. The shaded regions correspond to the Valsalva maneuver.
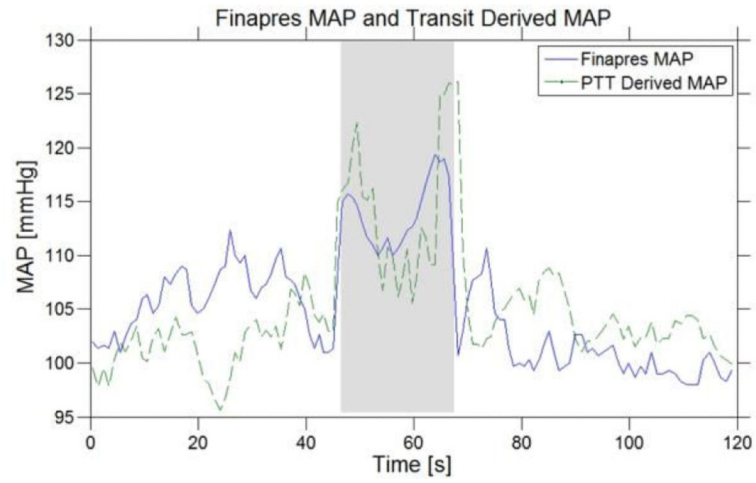
Fig. 6.
Finapres MAP and PTT derived MAP over a Valsalva maneuver. The gray shaded region corresponds to Valsalva strain. Mean error between the two waveforms is -0.07mmHg with a standard deviation of 3.64 mmHg.
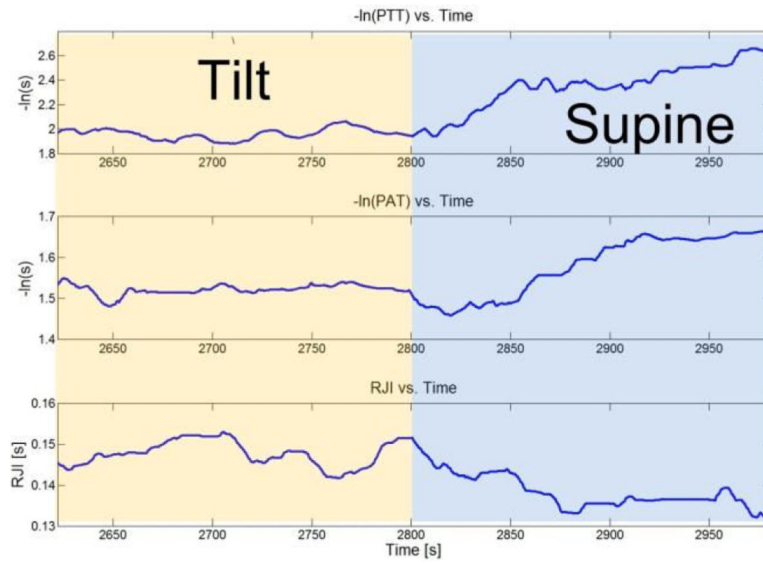
Fig. 7.
–ln(PTT), -ln(PAT), and R-J interval measured from the vital signs monitor during a tilt to supine maneuver.